Infrared and ab Initio Study of the Chloride−Ammonia Anion Complex

P. S. Weiser, D. A. Wild, P. P. Wolynec, and E. J. Bieske*

School of Chemistry, University of Melbourne, Parkville, Victoria 3052, Australia

Received: August 12, 1999; In Final Form: December 10, 1999

The infrared spectrum of the Cl^-−NH_3 anion complex has been recorded in the 2900−3450 cm^{-1} range by monitoring the infrared-induced production of Cl^- anion fragments in a tandem mass spectrometer. The spectrum features an intense band centered at 3140 cm^{-1}, which is shifted by 196 cm^{-1} to lower frequency with respect to the ammonia ν_1 band (3336.2 cm^{-1}). Two much weaker peaks are observed at 3270 and 3340 cm^{-1}. Ab initio calculations performed at the MP2(full)/aug-cc-pVTZ level indicate that the complex possesses a C_s proton-bound minimum-energy structure, and yield vibrational frequencies and intensities that accord with the infrared data. Barriers, calculated at the MP4SDTQ(full)/aug-cc-pVTZ//MP2(full)/aug-cc-pVTZ level, for ammonia inversion and turnstile exchange of the bonded proton, were determined to be 5.72 and 1.66 kcal/mol, respectively.

I. Introduction

Ion solvation is an issue of fundamental significance, playing a central role in a host of different chemical contexts. Recently, concerted experimental and theoretical studies have focused on characterizing small charged cluster systems with the goal of exploring the first few steps of ion solvation, and hopefully providing insights that extend to bulk situations. Earlier measurements of ligand bond enthalpies and entropies obtained using high-pressure mass spectrometry, ICR, and photoelectron techniques, have been supplemented by spectroscopic studies that have provided cluster vibrational frequencies and intensities, electronic band shifts, and rotational constants. Together, the experimental data and the results from increasingly sophisticated theoretical ab initio calculations, have led to the development of a more complete picture of the manner in which charged and neutral solvation entities interact.

Regarding anion complexes, the most recent spectroscopic and theoretical attention has been devoted to hydrated species, particularly small halide−water clusters.[1−9] Both theoretical and experimental results show that the halide−water microsolvation structures are critically dependent on the size of the halide ion and the relative strength of the water−water and halide−water bonds. For the larger halides (Cl^-,[1,2] Br^-,[3] and I^- [3−5]) the complexes appear to be such that the halide resides on the surface of a hydrogen-bonded water network, whereas for the fluoride ion, due to the stronger halide−water bond and the ion's small size, the water molecules are prevented from effectively hydrogen bonding to one another, so that the smaller complexes have interior solvation configurations where the fluoride ion is surrounded by water molecules.[7]

Our investigations have been directed toward anion clusters containing other than aqueous ligands. Recently measured infrared spectra of I^-−$(C_2H_2)_n$[10] and Cl^-−$(C_2H_2)_n$[11] clusters suggest that the smaller halide−acetylene complexes ($n \leq 6$) possess interior solvation structures such that a central halide ion is surrounded by roughly equivalent acetylene ligands that are bound end-on to the core.

* To whom correspondence should be addressed. E-mail: e.bieske@chemistry.unimelb.edu.au.

To extend our investigations of anion complexes containing nonaqueous solvent units, we have undertaken a combined infrared and ab initio examination of the Cl^-−NH_3 dimer. While this complex has been subject to prior theoretical attention[12,13] and has been experimentally characterized through its photoelectron spectrum,[13] to our knowledge there has been no prior infrared spectroscopic study. High-pressure mass spectrometry studies indicate that the chloride−ammonia bond energy (8.2 kcal/mol[12]) lies below the energies of the ammonia ν_1 and ν_3 vibrations, making the complex ideal for characterization through infrared vibrational predissociation spectroscopy.

The most sophisticated ab initio study on Cl^-−NH_3 was carried out to interpret the photoelectron spectra.[13] Using the CCSD method and a truncated ANO basis set,[14,15] it was found that the dimer possesses a C_s equilibrium structure such that the ammonia molecule is attached to the chloride anion by a near linear hydrogen bond (N−H−Cl angle of 167.8°), with a $Cl^-\cdots H$ separation of 2.363 Å.[13] The theoretical work was mainly concerned with determining the Cl^-−NH_3 equilibrium geometry and energy to help in the interpretation of the complexes' photoelectron spectrum, and no calculated vibrational frequencies or intensities were reported. To gain a clearer picture of the Cl^-−NH_3 complex, we have carried out ab initio calculations at the MP2/aug-cc-pVTZ level to determine geometries and energies for the potential minimum and several transition states, along with vibrational frequencies and intensities. Infrared spectra allow us to assess the accuracy of the calculations and to determine whether a proton-bound structure is likely. The spectroscopic signature of a hydrogen-bonded structure, where a proton is shared with the Cl^- base, would be the appearance of an intense band shifted significantly to lower frequency compared to the symmetric ν_1 and doubly degenerate ν_3 hydrogen stretch vibrations of the free ammonia molecule.

II. Theoretical Methods and Results

Methodology. Four stationary points (refer to Figure 1) of the 28-electron, closed-shell system, Cl^-−NH_3, were investigated at the Møller−Plesset second-order (MP2) level of theory using Dunning's augmented correlation-consistent polarized

10.1021/jp992863o CCC: $19.00
Published on Web 03/04/2000

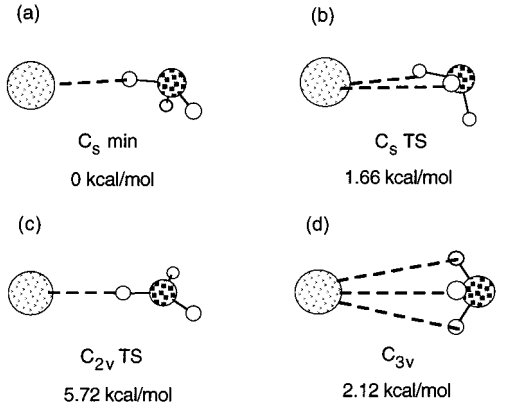

Figure 1. Geometries for stationary points of the $Cl^-−NH_3$ complex calculated at the MP2/aug-cc-pVTZ level of theory. Energy differences, with respect to the minimum energy C_s conformer, calculated at the MP4SDTQ/aug-cc-pVTZ level and corrected for vibrational zero-point energies, are provided in each case. Data for the four stationary points are given in Table 2. The transition states (b and c) are accessed, respectively, from the minimum-energy geometry (a) by a turnstile rotation of the ammonia with respect to the Cl^-, and the inversion of the ammonia ligand. The C_{3v} geometry, with three equivalent protons, corresponds to a second-order stationary point.

valence sets of triple-ζ quality (aug-cc-pVTZ).[16,17] All electrons were correlated. The basis set superposition error (BSSE) corrections to the binding energy were estimated using the counterpoise method of Boys and Bernardi.[18] Harmonic vibrational frequencies were computed analytically at the MP2(full) level of theory. The ab initio calculations were performed on a Cray J916 and a farm of DEC 600 workstations using the GAUSSIAN 94 suite of programs.[19]

Our choice of computational strategy was guided by earlier work on the $Cl^-−H_2O$ complex in which Xantheas[2] studied the hydration of the Cl^- anion at the MP2 and MP4 levels of theory, employing both the aug-cc-pVDZ and the aug-cc-pVTZ basis sets. It was found that the energetics and vibrational frequencies were more sensitive to the size of the basis set than to the order of the Møller−Plesset perturbation expansion, and that the MP2/aug-cc-pVTZ and MP4/aug-cc-pVTZ levels of theory yielded similar bond lengths and energetics. For example, using either basis set, the MP4 $Cl^-\cdots H_2O$ binding energies differed only slightly (<0.1 kcal/mol) from the corresponding MP2 results. In contrast, at the same order of Møller−Plesset expansion there were relatively large differences in binding energies using the larger aug-cc-pVTZ basis set compared to the aug-cc-pVDZ basis set. The success of the MP2/aug-cc-pVTZ level of theory in describing the essential features of the $Cl^-−H_2O$ complex has led to its use for the $Cl^-−NH_3$ calculations described in this paper. As the calculated energy differences between the various stationary points for the $Cl^-−H_2O$ complex were found to be small at the MP2/aug-cc-pVTZ level, we have also performed single-point MP4SDTQ/aug-cc-pVTZ energy calculations at the MP2/aug-cc-pVTZ geometries. Again, all electrons were correlated.

Theoretical Results. Calculated data for the free ammonia molecule and Cl^- anion are collected in Table 1. It can be seen that, where comparison between calculated and experimental values is possible, agreement is satisfactory. The N−H bond lengths are underestimated by 0.002 Å, while the bond angles are overestimated by 0.3°.

Geometries for the four stationary points of $Cl^-−NH_3$ are shown in Figure 1, and geometrical parameters, atomic charges, dipole moments, vibrational frequencies, and intensities are provided in Table 2. As in the earlier CCSD/ANO study,[13] the

TABLE 1: Calculated MP2/aug-cc-pVTZ Data for $^{35}Cl^-$, and the C_{3v} Minimum and D_{3h} Transition State of NH_3[a]

NH_3	C_{3v}	D_{3h}	exptl[b]
r(N−H) (Å)	1.010	0.994	1.012
θ(H−N−H) (deg)	107.0	(120.0)	106.7
$A = B$ (cm^{-1})	10.047	11.290	9.944
C (cm^{-1})	6.348	5.645	6.196
Q_N (au)	−1.032	−1.19	
Q_H (au)	0.344	0.370	
μ (D)	1.60	(0)	1.48
ω_1 (cm^{-1})	3534 (a_1) 3	3678 (a_1')	3336.2
ω_2 (cm^{-1})	1027 (a_1) 144	821i (a_1'')	932.5
ω_3 (cm^{-1})	3665 (e) 18	3885 (e′)	3443.6
ω_4 (cm^{-1})	1669 (e) 30	1599 (e′)	1626.1
zpe (kcal/mol)	21.77	20.94	
E_{MP2} (au)	−56.477491	−56.469955	
ΔE_{MP2} (kcal/mol)	(0.0)	4.73	
$\Delta E_{MP2,corr}$ (kcal/mol)	(0.0)	3.90	5.77[c]
E_{MP4} (au)	−56.498305	−56.490030	
ΔE_{MP4} (kcal/mol)	(0)	5.19	
$\Delta E_{MP4,corr}$ (kcal/mol)	(0)	4.36	5.77[c]
E (Cl^-) (au)	−459.814378		

[a] Included are internal geometries, rotational constants, natural charges on atomic centers, dipole moments, and vibrational frequencies and their associated infrared intensities(km/mol). For the C_{3v} minimum the vibrational frequencies are followed by the mode symmetry and infrared intensity. Also given are zero-point vibrational energies (zpe), electronic energies (E), and electronic energy differences (ΔE). ΔE_{corr} refers to electronic energy differences corrected for zpe. [b] From ref 20. Vibrational frequencies corresponding to the lower inversion level are given. [c] Reference 21.

minimum of the $Cl^-−NH_3$ complex was found to be the C_s conformer shown in Figure 1a, such that the ammonia molecule is attached to Cl^- by a near linear hydrogen bond. There are small differences between the geometrical parameters determined in the current work and those found in the earlier CCSD/ANO study.[13] For example, the calculated N−H−Cl angle of 171.4° is slightly larger than the CCSD/ANO value (167.8°), while the distance between the bonded proton and Cl^- of 2.290 Å is somewhat shorter than the CCSD/ANO value (2.363 Å).

The difference in the electronic energy for the C_s minimum of $Cl^-−NH_3$ and the Cl^- and NH_3 constituents is calculated to be 9.9 kcal/mol, comparing favorably with the CCSD/ANO theoretical result (8.3 kcal/mol[13]). When vibrational zero-point energy (zpe) and BSSE are taken into account, the MP2/aug-cc-pVTZ value is reduced to 7.7 kcal/mol, which is close to the binding energy determined from the photoelectron spectrum (8.3 kcal/mol) and the association enthalpy found through high-pressure mass spectrometry (8.2 kcal/mol[12]). The corresponding MP4/aug-cc-pVTZ value is 7.6 kcal/mol.

Complexation with Cl^- affects the ammonia geometry in a number of ways. Most obviously, the N−H bond length for the shared proton is elongated by 0.018 Å from the free ammonia value. Surprisingly there is also a slight lengthening (0.002 Å) of the non-hydrogen-bonded proton bond lengths. The calculations also indicate that the ammonia molecule moves slightly further from planarity in the complex (Tables 1 and 2). Changes in the hydrogen stretch frequencies and intensities show the usual trends for hydrogen bonding with a marked decrease in the frequency of the ν_2 stretching mode associated with the bound proton with respect to the free ammonia ν_1 and ν_3 modes (by −217 cm^{-1} compared to ν_1 in NH_3). There is also a pronounced increase in the infrared intensity for vibrational modes involving motion of the bonded proton. While the free ammonia ν_1 and ν_3 modes are predicted to have intensities of 3 and 18 km/mol, respectively, the ν_2 mode of the complex,

TABLE 2: Calculated MP2/aug-cc-pVTZ Data for Four Stationary Points of $^{35}Cl^-{-}NH_3$ Shown in Figure 1[a]

	C_s min	C_s TS	C_{2v} TS	C_{3v}
r(Cl−H$_b$) (Å)	2.290	2.795	2.257	3.053
r(N−H$_b$) (Å)	1.028	1.016	1.016	1.015
r(N−H$_t$) (Å)	1.012	1.012	0.995	
θ(Cl−H$_b$−N) (deg)	171.4		180.0	
θ(H−N−H) (deg)	104.6(2)	104.7(2)	120.7(2)	100.8
θ(H−N−H) (deg)	105.2(1)	99.1(1)	118.5(1)	100.8
A (cm^{-1})	8.800	8.072	11.438	6.841
B (cm^{-1})	0.136	0.135	0.136	0.134
C (cm^{-1})	0.135	0.134	0.134	0.134
Q_{Cl} (au)	−0.978	−0.997	−0.973	−0.999
Q_{H_b} (au)	0.418	0.372	0.439	0.352
Q_N (au)	−1.080	−1.064	−1.150	−1.058
Q_{H_t} (au)	0.320	0.317	0.342	
μ (D)	3.67	3.48	4.62	3.02
	1.58	1.31	(0)	(0)
ω_1 (cm^{-1})	3555 (a′) 27	3617 (a′)	3767 (a_1)	3511 (a_1)
ω_2 (cm^{-1})	3317 (a′) 558	3498 (a′)	3400 (a_1)	1240 (a_1)
ω_3 (cm^{-1})	1656 (a′) 17	1661 (a′)	1566 (a′)	121 (a_1)
ω_4 (cm^{-1})	1175 (a′) 84	1208 (a′)	170 (a′)	3587 (e)
ω_5 (cm^{-1})	365 (a′) 54	232 (a′)	638 (b_1)	1682 (e)
ω_6 (cm^{-1})	168 (a′) 24	135 (a′)	770i (b_1)	217i (e)
ω_7 (cm^{-1})	3629 (a″) 0.3	3563 (a″)	3868 (b_2)	
ω_8 (cm^{-1})	1699 (a″) 0.9	1656 (a″)	1632 (b_2)	
ω_9 (cm^{-1})	285 (a″) 17	270i (a″)	257 (b_2)	
zpe (kcal/mol)	22.66	22.26	21.87	22.03
E_{MP2} (au)	−516.307639	−516.304267	−516.298045	−516.303068
ΔE_{MP2} (kcal/mol)	(0.0)	2.12	6.02	2.87
$\Delta E_{MP2,corr}$ (kcal/mol)	(0.0)	1.72	5.23	2.24
E_{MP4} (au)	−516.351773	−516.348495	−516.341408	−516.347390
ΔE_{MP4} (kcal/mol)	(0.0)	2.06	6.51	2.75
$\Delta E_{MP4,corr}$ (kcal/mol)	(0.0)	1.66	5.72	2.12

[a] Provided are internal geometries, rotational constants, natural charges on atomic centers, dipole moments, and vibrational frequencies. For the C_s minimum each vibrational frequency is followed by the mode's symmetry and infrared intensity (km/mol). Also given are zero-point vibrational energies (zpe), electronic energies (E), and electronic energy differences (ΔE). ΔE_{corr} refers to electronic energy differences corrected for zero-point vbrational energy.

which involves stretching motion of the bonded proton, has a calculated intensity of 558 km/mol.

The complex possesses three vibrational modes corresponding to the relative motion of the ammonia and chloride constituents, the ω_6 intermolecular stretch mode (168 cm^{-1}, a′ symmetry), ω_5 intermolecular rock mode (365 cm^{-1}, a′ symmetry), and ω_9 intermolecular wag mode (285 cm^{-1} a″ symmetry). In all three cases the harmonic frequencies are all likely to be overestimations as the potential energy surface along the three intermolecular coordinates is highly anharmonic. For example, the ω_9 wag mode corresponds to the 3-fold internal rotation of the ammonia between the three equivalent C_s proton-bound minima, which has a barrier of only 600 cm^{-1} (Table 2).

The electronic populations on the atomic centers of the $Cl^-{-}NH_3$ anion complex (Tables 1 and 2) are of interest as they provide a guide to the degree of charge transfer and polarization accompanying complex formation. Natural charges are provided in Tables 1 and 2 as they are less dependent on basis set than those derived from a Mulliken analysis.[22] For the C_s minimum-energy conformer of $Cl^-{-}NH_3$ there is slight transfer of negative charge from the Cl^- to the ammonia molecule (0.022 au). Furthermore, as expected, the charge distribution within the ammonia molecule is polarized by the chloride anion, with an enhancement of the positive charge on the bonded proton (by 0.074 au) and a decrease of positive charge on the two nonbonded protons (by −0.024 au).

Regarding the transition states, it is found that when zero-point energy is taken into account the bifurcated C_s structure in which two equivalent protons are bound to the Cl^- (Figure 1b) lies 1.66 kcal/mol higher in energy than the minimum. Adoption of the bifurcated structure involves a substantial change in the ammonia geometry with a reduction of the $H_b{-}N{-}H_b$ angle to 99.1°. The planar C_{2v} structure (Figure 1c) is the transition state for inversion of the complex and lies 5.72 kcal/mol above the C_s minimum. Complexation leads to an *increase* in the inversion barrier compared to the free ammonia molecule (Tables 1 and 2). The C_{3v} geometry (Figure 1d) lies 2.12 kcal/mol higher in energy than the C_s minimum and is found to be a second-order stationary point, with a doubly degenerate imaginary frequency (ω_6(e) = 217i cm^{-1}) corresponding to a rocking motion toward one of the three equivalent protons.

III. Experimental Methods

The vibrational predissociation spectrum of $^{35}Cl^-{-}NH_3$ was recorded in a low-energy, guided ion beam apparatus.[10,11] The machine consists of an ion source, primary quadrupole mass filter for selection of the parent $^{35}Cl^-{-}NH_3$ complexes, a quadrupole bender that deflects the beam through 90° into a 60 cm long octopole ion guide, a secondary quadrupole mass filter for selection of the photofragment, and an ion detector. Under typical operating conditions the pressure in the octopole region is less than 10^{-7} Torr. While traveling through the octopole guide, the ions meet a counterpropagating IR beam, which when set to an appropriate wavelength, serves to excite the complexes to predissociative (ro)vibrational levels, resulting in $^{35}Cl^-$ photofragments. These fragment anions enter a secondary quadrupole mass filter and are subsequently detected by a microchannel plate coupled to a boxcar integrator. As the $Cl^-{\cdots}NH_3$ bond energy is approximately 2870 cm^{-1},[12] absorption of a single infrared photon across the 2900−3450 cm^{-1} scan range should be sufficient to cause photodecomposition to produce Cl^- and NH_3 fragments. The alternative $HCl + NH_2^-$

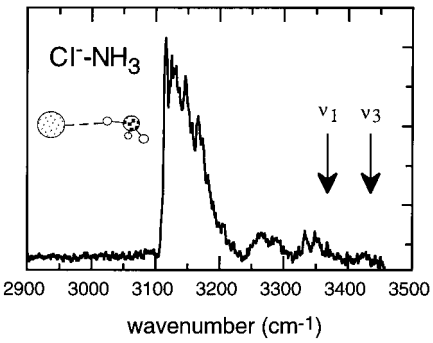

Figure 2. Midinfrared spectrum of the $Cl^-−NH_3$ anion complex in the 2900−3450 cm^{-1} range, obtained by recording the Cl^- photofragment signal. Positions of the free ammonia stretching vibrations (ν_1, 3336.2 cm^{-1}; ν_3, 3443.6 cm^{-1} [20]) are marked by arrows. Wavenumbers, widths, and assignments of the peaks are listed in Table 3.

TABLE 3: Infrared Peak Positions for the $Cl^-−NH_3$ Anion Complex in the 2900−3450 cm^{-1} Range, Including Wavenumbers for Infrared Absorptions, Estimated Bandwidths, Relative Intensities, and Assignments

wavenumber (cm^{-1})	bandwidth (cm^{-1})	rel intens	disp from ν_2 (cm^{-1})	assignment
3140 ± 10	60	100	0	ν_2
3270 ± 10	50	15	120	$(\nu_2 + \nu_6/(\nu_2 + \nu_5)$
3340 ± 10	45	10	190	ν_1

dissociation asymptote lies 3.05 eV higher in energy,[23] and should not be important in this study.

The $Cl^-−NH_3$ complexes were synthesized in an electron beam crossed supersonic expansion in an arrangement similar to the one described in ref 24. Ammonia gas seeded with CCl_4 was expanded from a pulsed nozzle (0.8 mm orifice diameter, 40 Hz repetition rate) and crossed by 200 eV electrons issued from twin tungsten filaments. The source design permits variation of the distance between the electron emitting filaments and nozzle orifice to maximize the $Cl^-−NH_3$ signal. It is probable that the complexes are formed either through intracluster dissociative attachment processes in preformed $(CCl_4)_m(NH_3)_n$ clusters downstream in the expansion, or through three-body association reactions between Cl^- and NH_3 molecules close to the nozzle.[25]

Tunable infrared light was produced using a Nd:YAG pumped optical parametric oscillator (OPO) capable of generating light in the 2500−6900 cm^{-1} range with a bandwidth of less than 0.02 cm^{-1}. Wavelength calibration was accomplished using a pulsed wavemeter (New Focus 7711), through measurements of the OPO oscillator wavelength and 532 nm output of the seeded Nd:YAG laser. The laser was run at half the frequency of the pulsed ion source so that laser-on/laser-off background subtraction could be employed to account for collisional and metastable fragmentation. While it is difficult to estimate the vibrational temperature of the anion complexes probed in this study, it is known that the ion source is capable of producing cation complexes with temperatures of roughly 40 K.[24]

IV. Experimental Results and Discussion

Figure 2 shows the infrared spectrum of $^{35}Cl^-−NH_3$ obtained by scanning the OPO over the 2900−3450 cm^{-1} range while detecting the $^{35}Cl^-$ photofragment signal. Band positions, widths, and assignments are given in Table 3. The spectrum is dominated by an intense peak centered at 3140 cm^{-1} with a head at 3115 cm^{-1}, and features two weaker peaks occurring at 3270 and 3340 cm^{-1}. Survey scans down to 2700 cm^{-1} failed to reveal other peaks.

The form of the infrared spectrum is consistent with the proton-bound C_s conformer shown in Figure 1a. The dominant 3140 cm^{-1} band can be convincingly assigned to the ν_2 band of the complex, which for the C_s conformer is predicted to be the most intense infrared transition. The band's 196 cm^{-1} shift to lower frequency with respect to the ammonia ν_1 band (3336.2 cm^{-1})[20] accords well with the calculated ν_2 shift of −217 cm^{-1} for the C_s structure (Tables 1 and 2).

The shape of the ν_2 band, with its pronounced head to lower energy, suggests that the intermolecular bond contracts upon excitation of the intermediate proton. Such a phenomenon has been observed for corresponding transitions in related proton-bound anion[10] and cation complexes[26−28] and indicates that vibrational excitation of the intermediate proton increases the effective attraction between the Cl^- and NH_3.

While definite assignments cannot be offered for the two smaller peaks, it appears likely that the peak at 3340 cm^{-1} (displaced by 190 cm^{-1} from the ν_2 band center) is associated with the ν_1 vibration (symmetric stretching motion of the two nonbonded protons), which according to the calculations should occur 238 cm^{-1} to the blue of the ν_2 band with roughly 5% its intensity. Although the signal-to-noise ratio for this transition is poor, the band appears to be more symmetrical than the ν_2 band, consistent with the notion that excitation of the nonbonded protons should have little influence on the effective intermolecular potential. The other minor peak at 3270 cm^{-1} (displaced from ν_2 by 120 cm^{-1}) is conceivably due to ν_2 in combination with one of the intermolecular modes. Analogous combination bands have often been observed for proton-bound cation complexes.[26−28] While the stretching and two bending intermolecular modes (ν_6, ν_5, and ν_9) are calculated to have harmonic frequencies of 365, 168, and 285 cm^{-1}, respectively, the actual values are likely to be somewhat lower due to anharmonicity. In this regard it is worth noting that the bifurcated C_s and the C_{3v} stationary points (Figure 1b, d) that are accessed by deformation of the complex along the ν_9 and ν_5 coordinates lie only 580 and 740 cm^{-1} above the C_s ground state.

The lack of resolved rotational features in the spectrum is at first sight puzzling given that the calculated $Cl^-−NH_3$ rotational constants are a lot larger than the laser bandwidth (0.02 cm^{-1}). While lifetime broadening may play some role in obscuring rotational features, there are also sources of heterogeneous broadening that may be important. If the $Cl^-−NH_3$ complex is approximated as a rigid, near prolate asymmetric rotor, then excitation of the ν_2 vibration should lead to a series of parallel $\Delta K = 0$ subbands, each with P and R branch lines spaced by approximately $B + C = 0.270$ cm^{-1} (assuming the rotational constants in Table 2). However, if the lower and upper state rotational constants differ, the $\Delta K = 0$ subbands will no longer overlap, resulting in spectral congestion for warmer complexes. Moreover, vibrational hot bands may be present, and these probably contribute to the ν_2 band's high-energy tail. Stiffening of the intermolecular bond in the upper vibrational state will result in the displacement of hot bands involving the intermolecular stretching and bending vibrations to higher energy compared to the fundamental vibration.

Additional complications will occur in the energy level structure and spectrum of $Cl^-−NH_3$ due to tunneling between the three equivalent hydrogen-bonded minima and the ammonia inversion. The importance of these effects in the $Cl^-−NH_3$ spectrum is difficult to estimate without conducting full rovibrational calculations for the ground and vibrationally excited state intermolecular potentials. Such calculations have been carried out for the $H^-−NH_3$ complex that has characteristics

similar to those of $Cl^-—NH_3$.[29] The equilibrium geometry is such that the H^- is attached to one of the ammonia hydrogen atoms. The well depth is 2661 cm^{-1} (7.6 kcal/mol), and the barrier for 3-fold tunneling is 1736 cm^{-1} (4.96 kcal/mol). The rovibrational calculations indicate that both the inversion and 3-fold tunneling motions are substantially quenched through complexation with the hydrogen-bonded H^-. The inversion doubling of the ammonia moiety is reduced from the free molecule value of 0.793 cm^{-1} to 0.0074 cm^{-1}, while the energy difference between the lowest ortho and para forms of the complex, which reflects the facility of 3-fold tunneling, is 0.393 cm^{-1}. Although the barrier for 3-fold internal rotation is smaller for $Cl^-—NH_3$ (1.66 kcal/mol), this motion will probably also be substantially quenched due to the large chloride mass. The chloride mass will also play a role in quenching the inversion motion, as will the enhanced tunneling barrier in the complex compared to the free molecule (Tables 1 and 2).

It is of some interest to compare briefly the properties of $Cl^-—NH_3$ with those of the isoelectronic $Cl^-—H_2O$ complex. In both cases the calculations show that an asymmetric equilibrium structure is preferred, such that a single proton is shared with the chloride ion with significant barriers to exchange of the bonded proton. High-pressure mass spectrometry studies show that the chloride−ammonia bond is somewhat weaker than the chloride−water bond (8.2 kcal/mol[12] vs 14.7 kcal/mol[30]), and this difference is reflected in the smaller vibrational band shift for $Cl^-—NH_3$. Taking the mean of the ammonia ν_1 and ν_3 vibrations as a reference point, the shift for $Cl^-—NH_3$ is −275 cm^{-1}, while for $Cl^-—H_2O$ the shift from the mean of the symmetric and antisymmetric water stretch vibrations is −580 cm^{-1}.[1,2] The stronger intermolecular interaction in the water-containing complex is also reflected in the larger Cl^--induced distortion of the $O—H_b$ bond compared to the $N—H_b$ bond (an increase of 0.3 Å for $Cl^-—H_2O$[2] vs 0.2 Å for $Cl^-—NH_3$).

Acknowledgment. We thank Prof. R. O. Watts and Prof. J. B. Peel for their generosity, R. J. Mathys and J. W. Nuske for technical assistance, the High Performance Computing Centre (HPCC) of The University of Melbourne and RMIT for allocation of computing resources, and the Australian Research Council and The University of Melbourne for financial support.

References and Notes

(1) Choi, J.-H.; Kuwata, K. T.; Cao, Y.-B.; Okumura, M. *J. Phys. Chem.* **1998**, *102*, 503.
(2) Xantheas, S. S. *J. Phys. Chem.* **1996**, *100*, 9703.
(3) Ayotte, P.; Bailey, C. G.; Weddle, G. H.; Johnson, M. A. *J. Phys. Chem.* **1998**, *102*, 3067.
(4) Johnson, M. S.; Kuwata, K. T.; Wong, C.; Okumura, M. *Chem. Phys. Lett.* **1996**, *260*, 551.
(5) Ayotte, P.; Weddle, G. H.; Kim, J.; Johnson, M. A. *Chem. Phys.* **1998**, *239*.
(6) Ayotte, P.; Weddle, G. H.; Kim, J.; Kelley, J.; Johnson, M. A. *J. Phys. Chem.* **1999**, *103*, 3,.
(7) Cabarcos, O. M.; Weinheimer, C. J.; Lisy, J. M.; Xantheas, S. *J. Chem. Phys.* **1999**, *110*, 5.
(8) Xantheas, S.; Dunning, T. *J. Phys. Chem.* **1994**, *98*, 13489.
(9) Xantheas, S. *J. Am. Chem. Soc.* **1995**, *117*, 10373.
(10) Weiser, P. S.; Wild, D. A.; Bieske, E. J. *Chem. Phys. Lett.* **1998**, *299*, 303.
(11) Weiser, P. S.; Wild, D. A.; Bieske, E. J. *J. Chem. Phys.* **1999**, *110*, 9443.
(12) Evans, D. H.; Keesee, R. G.; Castleman, A. W., Jr. *J. Chem. Phys.* **1987**, *86*, 2927.
(13) Markovich, G.; Cheshnovsky, O.; Kaldor, U. *J. Chem. Phys.* **1993**, *99*, 6201.
(14) Widmark, P. O.; Malmquist, P. Å.; Roos, B. O. *Theor. Chim. Acta* **1990**, *77*, 291.
(15) Widmark, P. O.; Persson, B. J.; Roos, B. O. *Theor. Chim. Acta* **1991**, *79*, 419.
(16) Dunning, J. T. H. *J. Chem. Phys.* **1989**, *90*, 1007.
(17) Kendall, R. A.; Dunning, J. T. H.; Harrison, R. J. *J. Chem. Phys.* **1992**, *96*, 6796.
(18) Boys, S. F.; Bernardi, F. *Mol. Phys.* **1970**, *19*, 553.
(19) Frisch, M. J.; Trucks, G. W.; Schlegel, H. B.; Gill, P. M. W.; Johnson, B. G.; Robb, M. A.; Cheeseman, J. R.; Keith, T.; Petersson, G. A.; Montgomery, J. A.; Raghavachari, K.; Al-Laham, M. A.; Zakrzewski, V. G.; Ortiz, J. V.; Foresman, J. B.; Cioslowski, J.; Stefanov, B. B.; Nanayakkara, A.; Challacombe, M.; Peng, C. Y.; Ayala, P. Y.; Chen, W.; Wong, M. W.; Andres, J. L.; Replogle, E. S.; Gomperts, R.; Martin, R. L.; Fox, D. J.; Binkley, J. S.; Defrees, D. J.; Baker, J.; Stewart, J. P.; Head-Gordon, M.; Gonzalez, C.; Pople, J. A. *Gaussian 94, Revision E.2*; Gaussian, Inc.: Pittsburgh, PA, 1995. NBO Version 3.1: E. D. Glendening, A. E. Reed, J. E. Carpenter, F. Weinhold.
(20) Herzberg, G. *Molecular Spectra and Molecular Structure Volume III, Electronic Spectra and Electronic Structure of Polyatomic Molecules*; Krieger: Malabar, FL, 1991; Vol. I.
(21) Swalen, J. D.; Ibers, J. A. *J. Chem. Phys.* **1962**, *36*, 1914.
(22) Reed, A. E.; Weinstock, R. B.; Weinhold, F. *J. Chem. Phys.* **1985**, *83*, 735.
(23) Lias, S. G.; Barmess, J. E.; Liebman, J. F.; Holmes, J. L.; Levin, R. D.; Mallard, W. G. *J. Phys. Chem. Ref. Data Suppl.* **1988**, *17*, 1.
(24) Bieske, E. J. *Faraday Trans.* **1995**, *91*, 1.
(25) Johnson, M. A.; Lineberger, W. C. In *Techniques for the Study of Ion−Molecule Reactions*; Farrar, J. M., Saunders, W. H. J., Ed.; Wiley: 1988; Vol. XX.
(26) Nizkorodov, S. A.; Maier, J. P.; Bieske, E. J. *J. Chem. Phys.* **1995**, *102*, 5570.
(27) Nizkorodov, S. A.; Maier, J. P.; Bieske, E. J. *J. Chem. Phys.* **1995**, *103*, 1297.
(28) Nizkorodov, S. A.; Dopfer, O.; Ruchti, T.; Meuwly, M.; Maier, J. P.; Bieske, E. J. *J. Phys. Chem.* **1995**, *99*, 17118.
(29) van der Sanden, G. C. M.; Reinsch, E.-A.; van der Avoird, A.; Wormer, P. E. S.; Rosmus, P. *J. Chem. Phys.* **1995**, *103*, 4012.
(30) Hiraoka, K.; Mizuse, S.; Yamabe, S. *J. Phys. Chem.* **1988**, *92*, 2923.